JOURNAL OF PROPULSION AND POWER
Vol. 9, No. 3, May–June 1993

Inlet Turbulence Distortion and Viscous Flow Development in a Controlled-Diffusion Compressor Cascade at Very High Incidence

G. V. Hobson* and R. P. Shreeve†
Naval Postgraduate School, Monterey, California 93943

Detailed two-component laser Doppler velocimeter (LDV) measurements of the flow through a controlled-diffusion (CD) compressor cascade at a Reynolds number of about 700,000 and at a low Mach number are reported in this article. A very high-incidence angle (8 deg above design) was considered throughout this investigation, which included the full experimental characterization of the turbulence field. The LDV measurements were fully automated and were all taken in coincidence mode, thus turbulent flow correlations could be determined. Most significant was the measurement of the distortion of the inlet freestream turbulence upstream of the blade leading edges. Such information is important in assessing viscous codes which incorporate transport equations to describe the turbulence within the flowfield. The laminar leading-edge separation bubble, which reattached turbulent, was enlarged on the suction surface of the blade. Consistent with measurements at lower incidence angles, the suction surface boundary layer remained attached over the rear part of the blade. The pressure side boundary layer initially showed little or no growth, however, it finally developed into a profile similar to a wall jet. The wake profiles showed significant asymmetry due to the high loading on the blades at the increased incidence angle.

Nomenclature

C_p = pressure coefficient
c_{ij} = correlation coefficient $\overline{u'v'}/[\overline{u'^2v'^2}]^{1/2}$
p = static pressure
Tu = turbulence intensity, $[\overline{u'^2}]^{1/2}/U$
t = time, Eq. (1)
$\mathcal{T}$ = integral scale
U = pitchwise mean velocity component
U' = mean velocity component at 135 deg
$Utot$ = total mean velocity
u' = fluctuating component of U
V = axial mean velocity component
V' = mean velocity component at 45 deg
$Vref$ = reference, upstream total velocity
v' = fluctuating component of V
x = pitchwise direction, Fig. 1
y = axial direction, Fig. 1
z = spanwise direction, Fig. 2
β = air angle, Fig. 1
λ_f = characteristic length scale
ρ = density
$\rho(\tau)$ = autocorrelation coefficient
τ = delay time
τ_{ij} = Reynolds stress, $-\overline{\rho u'v'}$

Subscripts
1 = upstream
2 = downstream

Introduction

THE need to predict off-design and stalling behavior of compressor blade elements for design purposes has resulted in extensive experimental studies to map viscous flow development in specific geometries. Recently, Elazar and Shreeve[1] reported a two-component LDV mapping of the flow through the subsonic CD cascade at three incidence angles. This followed a study by Deutsch and Zierke[2–4] of the boundary-layer behavior in a double-circular-arc (DCA) compressor cascade using a single component LDV system. These two studies have provided basic, but contrasting, test cases for the computational fluid dynamic (CFD) simulation of flow through compressor blading.[5–8] In the case of the DCA blading, unsteady separation was found on the suction surface ahead of the trailing edge. In the CD blading, the flow was always attached to the trailing edge at all incidence angles, but the leading-edge separation bubble grew progressively as the incidence was increased.

Fully successful simulation of such test cases hinges on the modeling of transition and turbulence. However, if higher-order turbulence models are used, then a full comparison cannot be made without detailed measurements of the development of the turbulence field throughout the cascade. To properly establish the inlet boundary conditions for the simulation, it is important to measure the turbulence development upstream of the cascade. This was the motivation for the present study in which the flowfield through the CD cascade was extensively surveyed at a fixed incidence angle which was 2 deg greater than the highest incidence reported by Elazar and Shreeve.[1] A larger number of samples were used than in the previous work to ensure that the turbulence quantities were accurately obtained from statistical averaging of the data. An interesting development was that some measurements of forward moving seed particles were obtained for the first time within the separation bubble. This leading-edge separation bubble was found to be larger than in the previous studies. As was the case at lower incidence angles, the suction side boundary layer remained attached at the blade trailing edge.

Test Facility and Instrumentation

Low-Speed Cascade Tunnel

The subsonic cascade wind tunnel and operating instrumentation were as described by Sanger and Shreeve.[9] The

Presented as Paper 91-2004 at the AIAA/SAE/ASME/ASEE 27th Joint Propulsion Conference, Sacramento, CA, June 24–26, 1991; received July 30, 1991; revision received Sept. 21, 1992; accepted for publication Dec. 18, 1992.
*Associate Professor, Turbopropulsion Laboratory. Member AIAA.
†Professor, Turbopropulsion Laboratory. Member AIAA.

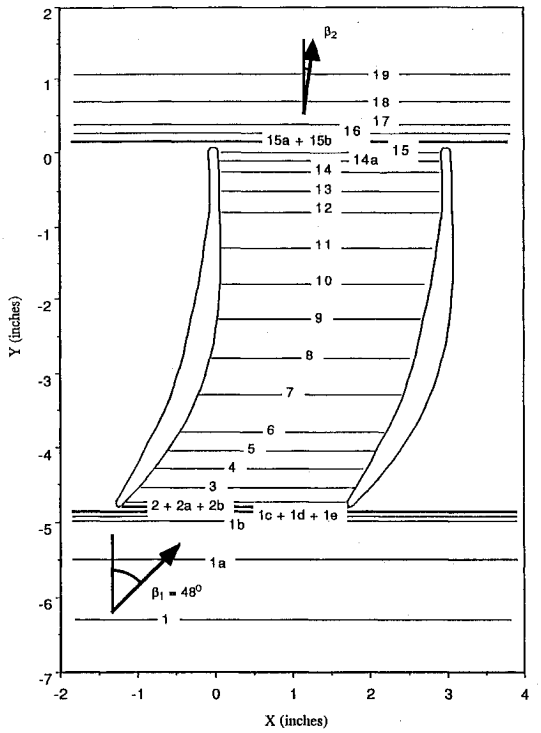

Fig. 1 Blade geometry and measurement stations.

cascade has 20 blades, the flow Reynolds number, based on chord length, was 7×10^4, and the inlet air angle was 48 deg. Inlet freestream turbulence intensities, as a result of the guide vanes upstream of the blades, were measured to be 1.5%.

The blades had a chord length of 5.01 in. and a spacing of 3 in., as shown in Fig. 1, which shows the blade passage and pitchwise locations where all the surveys were carried out. The blade coordinates and cascade geometry are reported by Elazar and Shreeve.[1]

Blade surface static pressure measurements were recorded with a 48-channel Scanivalve, and the inlet turbulence intensity, power spectrum, and autocorrelation were measured with a one-component TSI intelligent flow analyzer (IFA) (hot-wire) system. Standard single sensor hot-wire probes were used. The viscous flow development was measured using a fully automated TSI LDV system, as described by Murray.[10]

Experimental Procedure

Cascade Tunnel Setup

The inlet flow angle was set by adjusting the guide vanes and inlet walls. The exit flow angle was adjusted by setting the tailboards at angles which gave nearly uniform downstream wall static pressure measurements in the pitchwise direction across the cascade. The average inlet flow angle was measured, with the LDV, over three passage widths 31.3% of an axial chord length upstream of the blade leading edge.

Tunnel Calibration

The tunnel reference velocity (*Vref*) was determined using the analysis of Elazar.[11] At different tunnel speeds, the inlet flow velocity was measured (31.3% axial chord upstream) with the LDV, and the ambient pressure and temperature and the plenum total pressure and temperature were recorded. A least-squares curve fit was applied to the data to determine the calibration curve. During each subsequent run, the plenum and atmospheric conditions were recorded and used as input to a Newton method iteration algorithm to determine *Vref*.

Inlet Surveys

All LDV measurements presented in this article are averaged over 3000 data points, and no editing of the histograms was performed. Olive oil was used as a seed material in a TSI atomizer which produced approximately 1-μm size particles as measured by Elazar.[11]

The initial pitchwise survey at station 1 was conducted over three passage widths to determine the flow periodicity. All subsequent inlet pitchwise surveys were traversed over a 4-in. distance, spanning the region of maximum seeding. The seeding wand was adjustable, however, the adjustment was done on an arc, perpendicular to the tunnel, thus the seeding was not always at midspan. This limited the distance over which the pitchwise surveys could be extended. The first two inlet surveys, at stations 1 and 1a, were carried out with the laser horizontal. Station 1a was repeated with the laser pitched upwards by 4 deg. The need for pitching was to allow for closer access to the leading edge, i.e., so that there would not be any blade shadow interference at the subsequent stations 1b–e. At any time during the experiment if the laser was either pitched or yawed, then the previous survey would be repeated to enable the determination of any errors due to the measurement volume orientation. The maximum spatial error, due to probe volume orientation, was calculated to be 0.3 mm, which was the minimum diameter of the measurement volume. This error was because the probe volume was not parallel to the blade span, and therefore, seed particles displaced from the actual measurement location could be measured. The location of the measurement volume was always referenced to the same location between the blades throughout this experiment, the procedure is described by Elazar.[11] The correction for off-axis angular error resulted in an accurate comparison between the horizontal LDV measurements and the pitched LDV measurements.

The LDV orientation of 4-deg pitch was determined after experimenting at various angles. The beams converged at 3.1 deg, and a significant dropoff in the data rate was measured at a LDV pitch angle of 3 deg, which was attributed to the reflection of the beams from the tunnel window straight back into the optics. This effect had not been reported previously, and it was therefore decided to try to optimize the data rate and not incur too large a spatial error due to the LDV orientation. This resulted in the choice of 4 deg.

Passage Surveys

The passage surveys (between blades 7 and 8) were conducted with four different laser configurations.

1) The suction side close to the leading edge was surveyed from stations 2 and 7. The LDV was yawed by 4 deg to the left and pitched upward by 2 deg to avoid the laser beams being shadowed by the blade.

2) The LDV was yawed by 4 deg to the right and pitched downwards by 2 deg to access the pressure side of the blade close to the leading edge. All surveys from stations 1 to 7 were conducted with the LDV optics "standard," i.e., the 488-nm blue beam measuring the horizontal velocity component, and the 514.5-nm green beam measuring the vertical velocity component.

3) The optics were rotated by 45 deg and the LDV was yawed by 4 deg to the left to access the suction side of the blade from station 7 to 15. All subsequent measurements were carried out with the optics rotated with the green beam measuring V' and the blue beam U'. Suitable frequency shifting (which was kept at a constant magnitude of 1 MHz) changes had to be made so that the shifting was always in the same direction as the flow.

4) The LDV was yawed to the right by 4 deg to access the pressure side at the rear of the blade.

At each station within the passage, a complete survey comprised two different surveys, each originating from the adjacent blade surfaces and overlapping in the midpassage re-

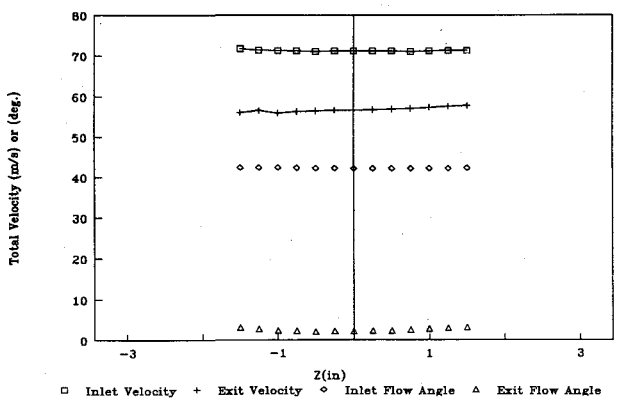

Fig. 2 Spanwise surveys.

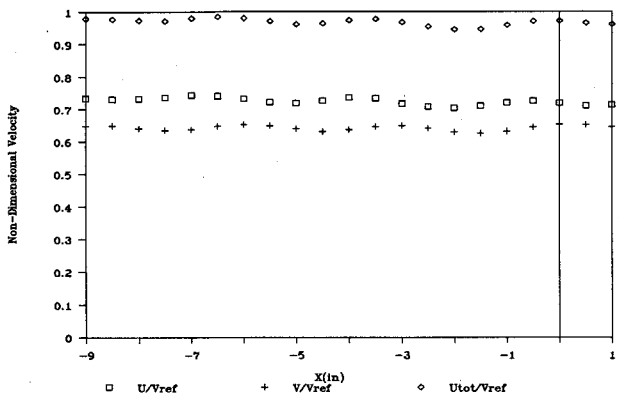

a) Mean velocity

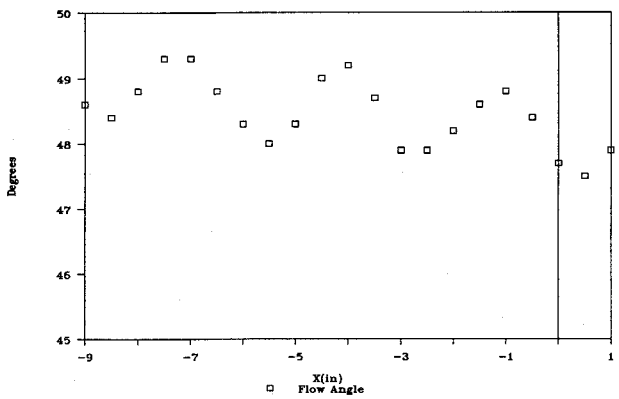

b) Flow angle

Fig. 3 Inlet pitchwise survey (over three passage widths).

gion. All surveys were initiated from the first location off the blade surface which gave a minimum data rate of 10 samples/s. The subsequent traverse points were stretched from the surface by a factor of 1.2. Because the adjacent surveys were carried out as much as one month apart, it was necessary that the tunnel was run within a plenum pressure tolerance of less than 1% to ensure good matching of the velocity profiles at midpitch, even though tunnel corrections were being applied.

Wake Surveys

Surveys at stations 15a and 15b were made behind blade 7, and the LDV was pitched downwards by 4 deg to access those locations close to the trailing edge. Surveys at stations 16–19 were completed over two passage widths with the LDV horizontal.

Periodicity and Two-Dimensionality

No end-wall suction was employed during this investigation, so the two-dimensionality of the flow upstream and downstream of the blades near the blade midspan had to be verified.

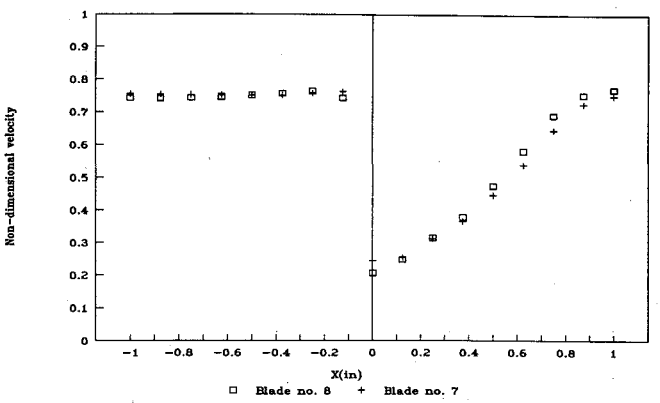

Fig. 4 Blade wake surveys (two wake profiles); mean velocity.

In Fig. 2, the results of spanwise surveys about the midspan are presented at the inlet (31.3% axial chord upstream) and exit (22.2% axial chord downstream). The seeding arrangement only allowed spanwise surveys of ±1.5 in., over which the flow was uniform both in magnitude and direction.

The inlet pitchwise flow distribution was determined over three blade passages to verify inlet flow uniformity and periodicity. The periodic upstream influence of the blades on the flow uniformity was evident at this location. There was about a 3% variation in magnitude of the total velocity (Fig. 3a) and the flow angle (Fig. 3b). The slight decrease in velocity magnitude and flow angle with increasing X, which was also evident in the endwall static pressure distribution, was felt to be acceptable.

A downstream periodicity check was performed by surveying the wakes of blades 7 and 8. The superposition of these profiles is presented in Fig. 4 which shows good repeatability of the mean velocity.

Results and Discussion

Blade Surface Pressure Distribution

The surface static pressure distribution as measured on blade number 10, which was fully instrumented with pressure taps, is presented in Fig. 5. In comparison to the pressure distribution for the lower incidence test cases, the blade is more highly loaded, and the loading has shifted towards the leading edge. The pressure gradient, on the suction side, does not level off between 10–30% chord as in the previous cases, but shows a steady increase in pressure over most of the suction surface. Towards the trailing edge, however, the pressure gradient levels off, which is a precursor of flow separation. The pressure surface static pressure distribution shows almost the same behavior as at all previous incidence angles.

Inlet Turbulent Power Spectrum, Autocorrelation, and Length Scale

In an attempt to characterize the inlet freestream turbulence, a hot wire was used to measure the inlet flow two chord lengths upstream of the blades. The turbulence intensity (1.5%) corresponded to that measured by the LDV. In addition to the above measurements of turbulence intensity, both the power spectral density and the autocorrelation of the streamwise component of the turbulence were recorded. The autocorrelation coefficient of a fluctuating function $u(t)$ depends only on the time difference $\tau = t' - t$, and is defined in Tennekes and Lumley[12] as

$$\rho(\tau) = [\overline{u(t)u(t')}/U^2] \tag{1}$$

where τ is a variable "delay" time and the product is averaged over t. $\mathcal{T}$ is defined by

$$\mathcal{T} = \int_0^\infty \rho(\tau)\, d\tau \tag{2}$$

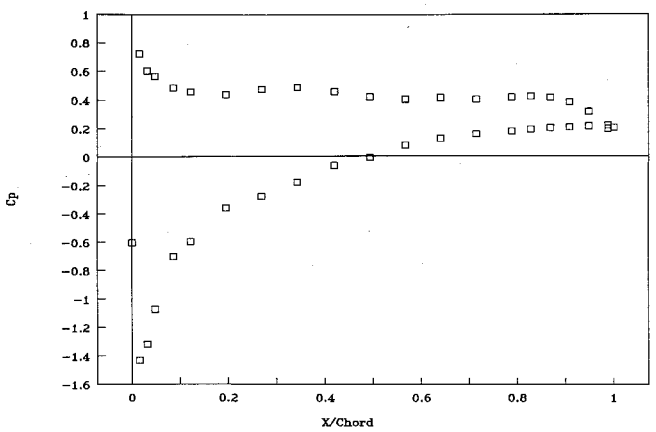

Fig. 5 Pressure coefficient distribution.

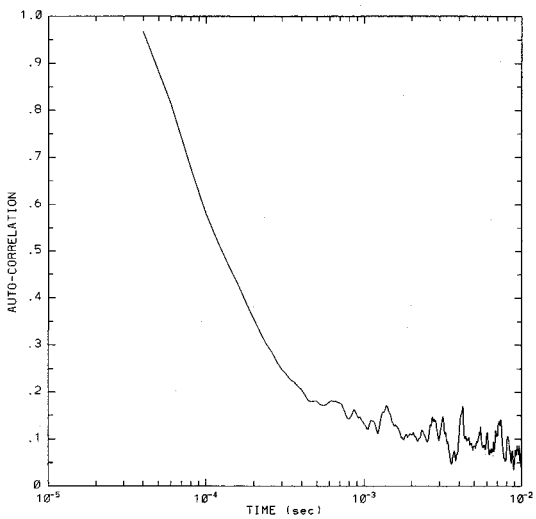

Fig. 6 Hotwire measurements of the inlet turbulent autocorrelation.

The value of $\mathcal{T}$, which is always assumed to be finite, is a rough measure of the interval over which $u(t)$ is correlated with itself. From Taylor's hypothesis, as presented by Hinze,[13] if $u'/U << 1$, then the turbulent eddies retain an approximate constant shape as they pass by the fixed hot-wire sensor. Then the autocorrelation is approximately equal to a space correlation with separation $U\tau$ in the x direction:

$$\rho(x) = \rho(U\tau) \tag{3}$$

Using Eqs. (2) and (3), a "characteristic" length scale, the streamwise integral scale λ_f, can be determined from

$$\lambda_f = U\mathcal{T} \tag{4}$$

The autocorrelation which was measured is presented in Fig. 6, which shows the distribution of the coefficient over 0.01-s time interval. The integral scale was determined to be 24 mm.

The power spectrum of the turbulence was typical of a freestream turbulence power spectral density distribution. The distribution was similar to the von Karman theoretical spectrum for one-dimensional isotropic turbulence, the form of turbulence expected to result in the flow "far" from the turbulence generating grids (in this case the inlet guide vanes). Unfortunately the high-frequency limit could not be measured because of a 20-MHz limitation of the TSI IFA 200 digitizer.

Inlet Pitchwise Surveys

The inlet velocity and turbulence intensity distributions are shown in Figs. 7a and 7b. A near uniform level of turbulence intensity of 1.5% was measured for both velocity components.

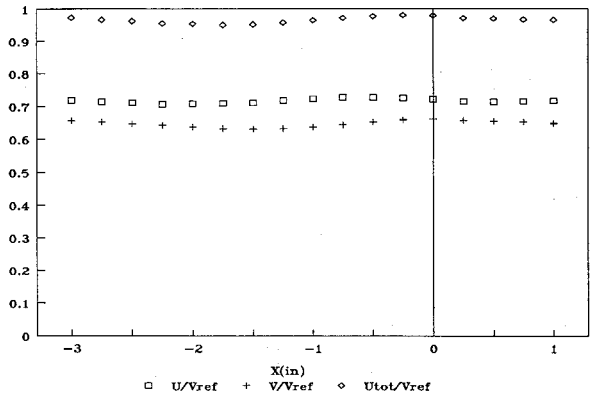

a) Mean velocity

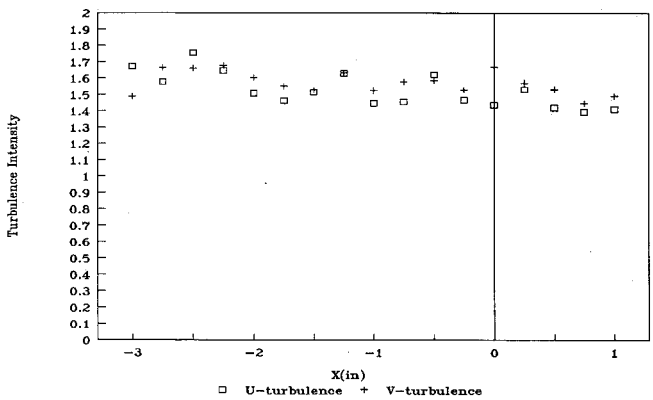

b) Turbulence intensities

Fig. 7 Inlet pitchwise survey at station 1.

This indicates that the turbulence was isotropic and that the wakes from the inlet guide vanes had fully mixed out at this axial station (31.3% upstream).

At station 1d, which is 1% of chord upstream of the leading edge, the mean flow was distorted considerably, as shown in Fig. 8a, with as much as a 50% variation in the total velocity across the passage. The turbulence intensity shown in Fig. 8b, in the region of the stagnation streamline, was increased by as much as an order of magnitude, and a breakdown in the periodicity of the turbulence is evident. The Reynold stress in this region, as shown in Fig. 8c, was negative on the pressure side and positive on the suction side.

Passage Surveys

Mean flow results are presented in Fig. 9a for the passage measurements at station 3 (5.2% of chord aft of the leading edge), which was within the leading-edge separation bubble. Only forward moving seed particles were measured in the "bubble" region, resulting in the positive velocity distribution close to the suction surface (at zero nondimensional passage width). Three possible explanations for this phenomena are suggested. First, the flow is unsteady in this region and the separation bubble may not always be present, thereby resulting in forward moving particles when the bubble is absent. Second, as pointed out by Johnson,[14] the flow in this region is locally three-dimensional, and therefore the separation may be rolling up into streamwise vortices (surface oil-film visualization seemed to indicate this). Third, only particle trace analysis will determine this, the seed particles may not follow the flow in this region of significant streamwise acceleration and deceleration. The flow unsteadiness was shown by the significant increase in turbulence intensity, in the free shear layer of the separation bubble, as seen in Fig. 9b.

Measurements at station 7 are shown in Fig. 10. By station 7, 31.3% axial chord aft of the leading edge, the flow was

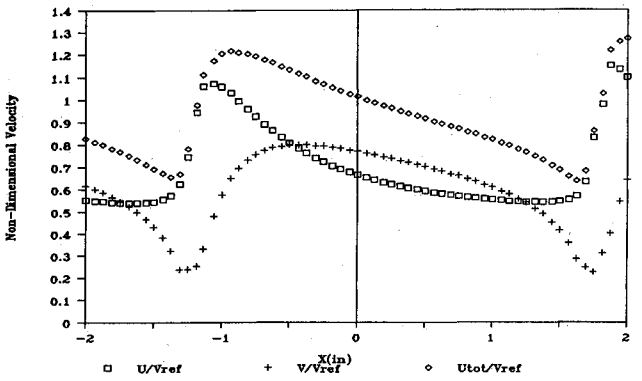

a) Mean velocity

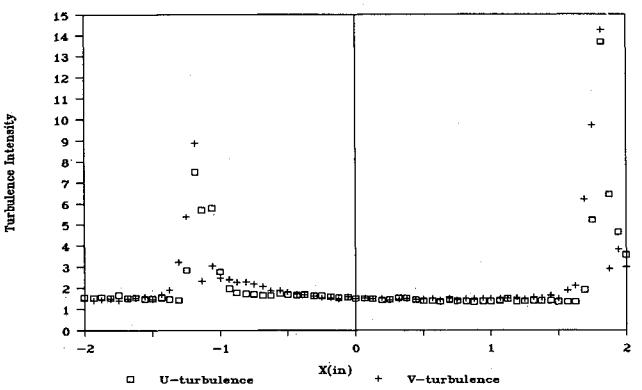

b) Turbulence intensities

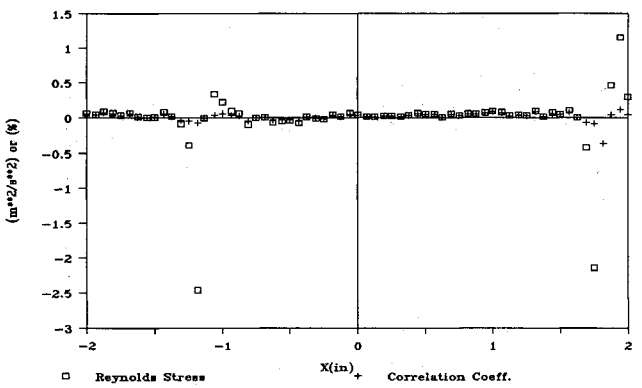

c) Reynolds stress

Fig. 8 Inlet pitchwise survey at station 1d.

reattached turbulent and the growth of the suction surface boundary layer extended to 15% of the passage width. Of note here is a measurement anomoly in the pressure side boundary layer. The measuring volume orientation may have biased the measurements toward the high-speed range, and there was noticeable scatter in the data in this region that also appeared as a significant increase in the turbulence intensity (Fig. 10b). At station 7 the optics were rotated by 45 deg, and all subsequent measurements were carried out with the same beam orientation.

At the trailing edge the passage survey was normal to the blade surfaces, thus it could also be interpreted as a boundary-layer survey. The results are shown in Fig. 11a. The suction side boundary layer has grown to 30% of the passage width, but remained attached. The pressure side boundary layer has developed as a wall jet which covered 5% of the passage width. The turbulence intensity increased to 12% on the U' component, and above 9% on the V' component at about 20% passage width. This shows the anisotropy of the turbu-

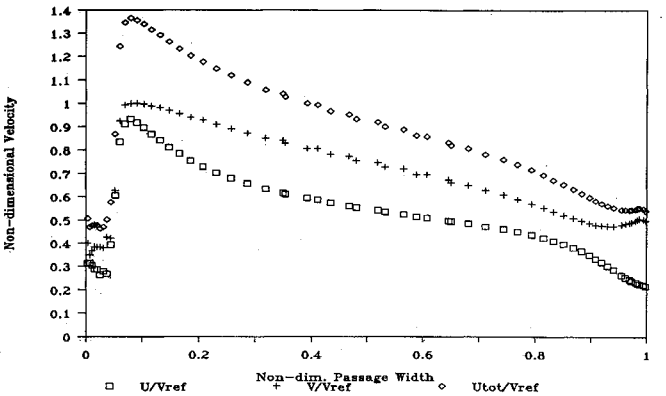

a) Mean velocity

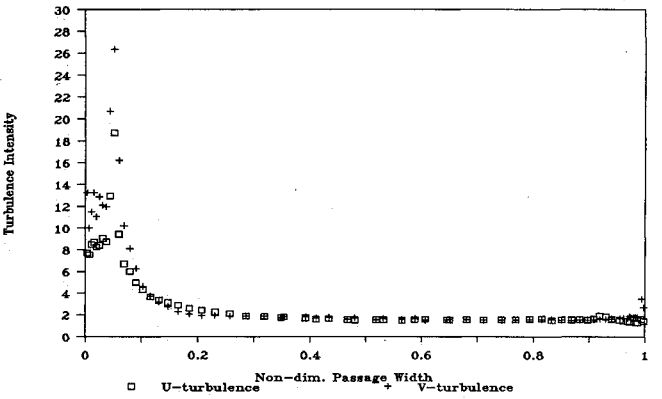

b) Turbulence intensities

Fig. 9 Passage survey at station 3.

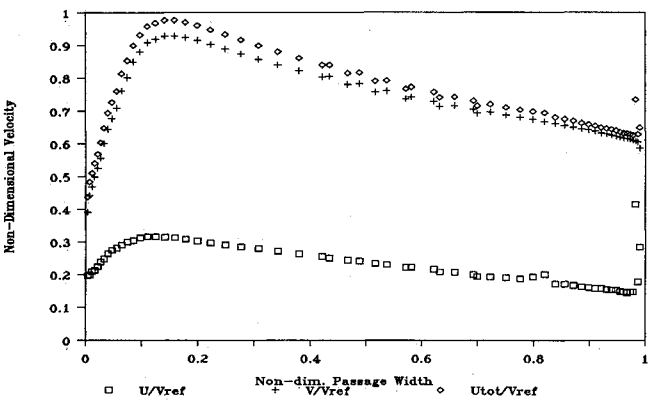

a) Mean velocity

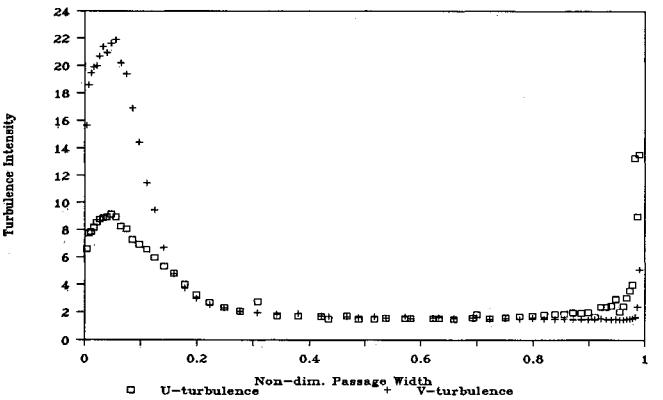

b) Turbulence intensities

Fig. 10 Passage survey at station 7.

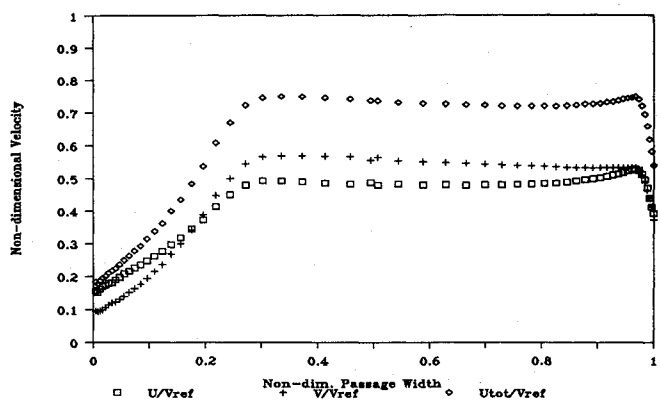

a) Mean velocity

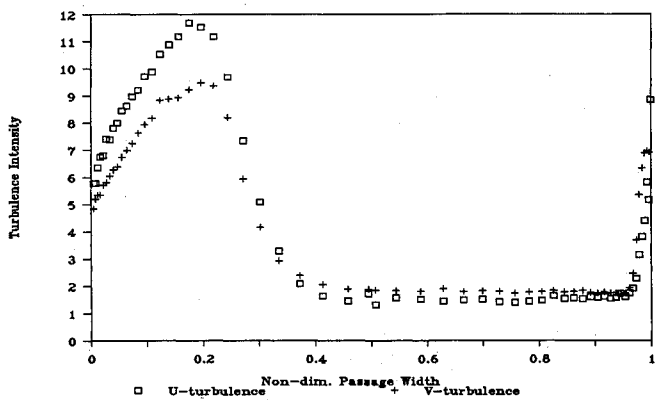

b) Turbulence intensities

Fig. 11 Passage survey at station 15.

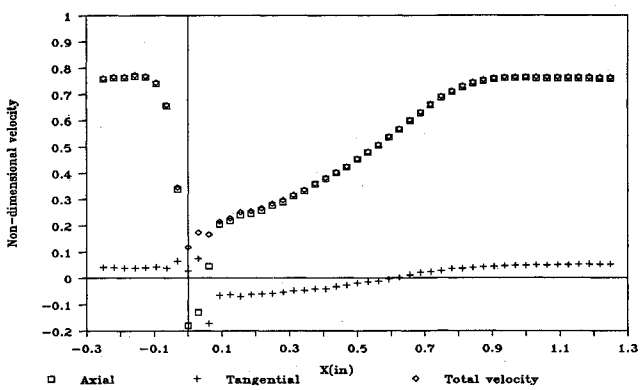

a) Mean velocity

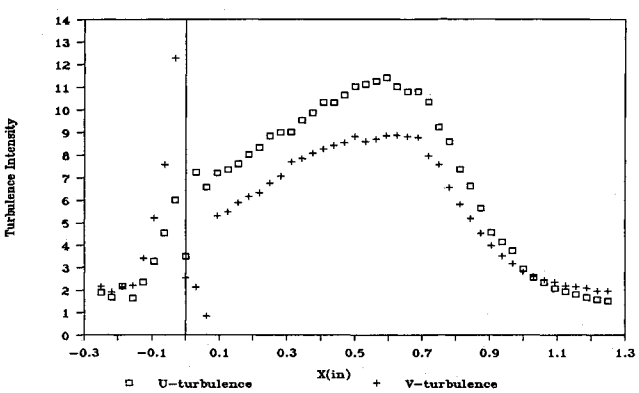

b) Turbulence intensities

Fig. 12 Wake survey at station 15b.

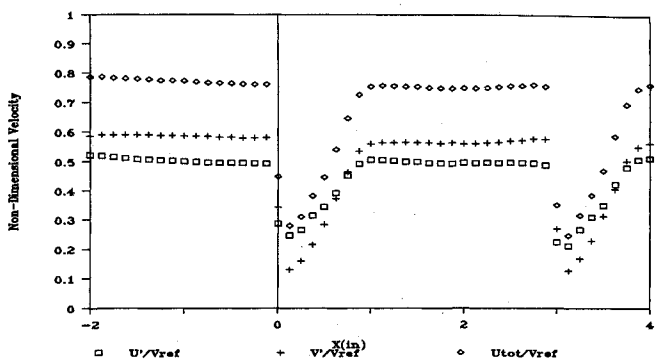

a) Mean velocity

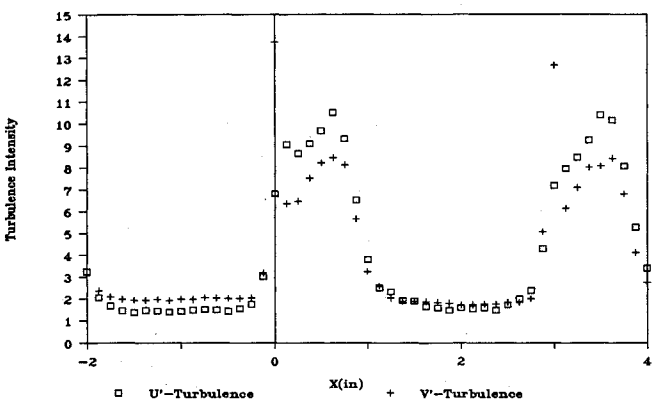

b) Turbulence intensities

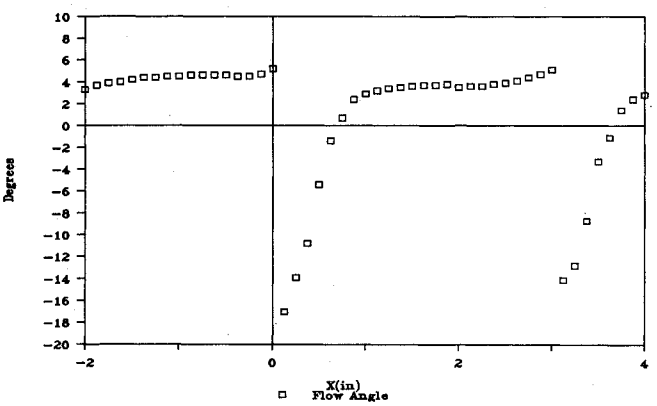

c) Flow angle

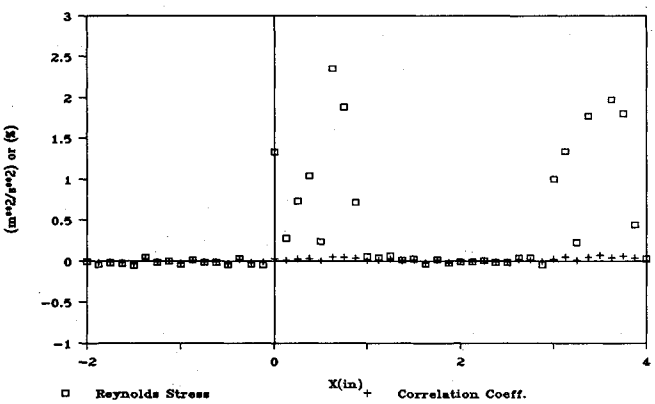

d) Reynolds stress

Fig. 13 Wake survey at station 18.

lence in the boundary layer. The turbulence intensity in the inviscid region had not increased significantly from the inlet value of 1.5%, as shown in Fig. 11b.

Wake Surveys

Although the suction side boundary layer was attached at station 15, the flow did separate from the blunt trailing edge (most probably into two recirculation regions). The wake measurements at 3% axial chord downstream of the trailing edge, shown in Fig. 12a, shows this flow reversal. The measured velocity components have been transformed into axial and tangential components. As shown, two locations (at X = 0.0 and 0.03 in.) had reverse mean flow velocities. The associated turbulence intensity distribution is given in Fig. 12b, which shows the asymmetry of the wake.

The reversed flow in the wake region had mixed out by station 16 (5% axial chord downstream). A complete set of data are presented further downstream at 14.15% axial chord downstream of the blades, in Figs. 13a–d. The time mean velocity distribution (Fig. 13a) shows an asymmetric wake and good periodicity. Periodicity was not reproduced in the turbulence field as shown in Fig. 13b, particularly on the U' component. The turbulence was anisotropic in the wake region and also in the inviscid region of the adjacent passage (behind blades 6 and 7). Periodicity was also somewhat lost in the exit flow angle distribution (Fig. 13c). For completeness, the Reynolds stress and correlation coefficient distribution are shown in Fig. 13d, which is positive across the wake.

Complete Flowfield Measurements

Finally, in summary, the complete flowfield which was measured with the LDV is presented as a vector plot in Fig. 14. Of note here is the significant acceleration of the flow over the suction surface at the leading edge, giving rise to the suction pressure shown in Fig. 5. Also of significance is the amount of entrainment of the flow into the suction surface boundary layer which continues in the wake. This entrainment should give rise to a static pressure distribution in the streamwise direction in the wake. It is felt by the authors that any computational validation of these results will have to accurately predict the entrainment effect and the pressure rise. This is particularly important if accurate predictions of the losses are to be obtained. The importance of accounting for the static pressure changes in the blade wake when deriving losses from LDV measurements alone has been described recently by Shreeve et al.[15]

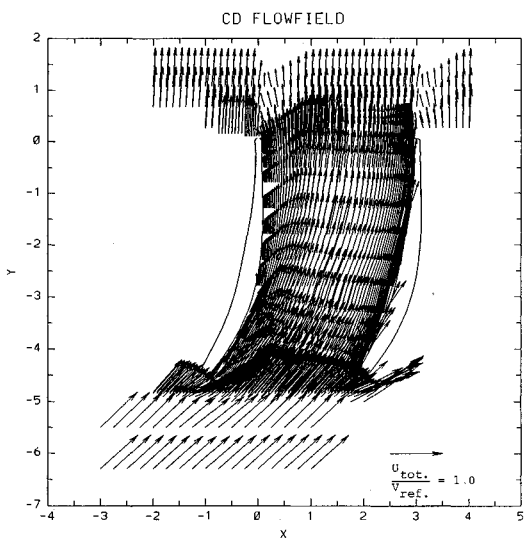

Fig. 14 Complete flowfield mean velocity vector plot.

Conclusion

At this very high-incidence angle, the laminar leading-edge separation bubble, which reattached turbulent, was enlarged. Although LDV measurements were taken in the bubble region, only forward moving particles were measured. Possible reasons have been given.

Consistent with earlier measurements at lower incidence angles, the suction surface boundary layer remained fully attached over the rear part of the blade. The pressure side boundary layer initially showed little or no growth. The flow profile near the trailing edge on the pressure side resembled a wall jet velocity profile.

Flow reversal was measured in the near wake. Further downstream of the blades, the wake profiles showed significant asymmetry.

Of most significance was the measurement of the distortion of the inlet freestream turbulence which occurred upstream of the blade leading edges. For viscous code assessment, this information is essential if transport equations are used to calculate the turbulence field through the cascade. If the increase in turbulence intensity is not accurately predicted, neither the subsequent development of the blade surface boundary layers nor the occurrence of separation can be accurately computed.

Finally, the authors will furnish a diskette containing the processed LDV measurements (in a form similar to those presented in this article) for all the measurement stations. These data will be furnished upon written request.

Acknowledgment

The present study was supported by the Naval Air Systems Command as part of the Air Breathing Propulsion Research Program under George Derderian.

References

[1]Elazar, Y., and Shreeve, R. P., "Viscous Flow in a Controlled Diffusion Compressor Cascade with Increasing Incidence," Gas Turbine and Aeroengine Congress and Exposition, American Society of Mechanical Engineers 89-GT-131, Toronto, Canada, June 4–8, 1989.

[2]Deutsch, S., and Zierke, W. C., "The Measurement of Boundary Layers on a Compressor Blade in Cascade: Part 1—A Unique Experimental Facility," *Journal of Turbomachinery*, Vol. 109, No. 4, 1987, pp. 520–526.

[3]Deutsch, S., and Zierke, W. C., "The Measurement of Boundary Layers on a Compressor Blade in Cascade: Part 2—Suction Surface Boundary Layers," *Journal of Turbomachinery*, Vol. 110, No. 1, 1988a, pp. 138–145.

[4]Deutsch, S., and Zierke, W. C., "The Measurement of Boundary Layers on a Compressor Blade in Cascade: Part 3—Pressure Surface Boundary Layers and the Near Wake," *Journal of Turbomachinery*, Vol. 110, No. 1, 1988b, pp. 146–152.

[5]Kirtley, K. R., and Lakshminarayana, B., "Computation of Internal Incompressible Separated Flow Using a Space-Marching Technique," AIAA 18th Fluid Dynamics and Plasmadynamics and Lasers Conf., AIAA Paper 85-1624, Cincinnati, OH, June 16–18, 1985.

[6]Liu, J-S., Sockol, P. M., and Prahl, J. M., "Navier-Stokes Cascade Analysis with a Stiff k-ε Turbulence Solver," AIAA 26th Aerospace Sciences Meeting, AIAA Paper 88-0594, Reno, NV, Jan. 11–14, 1988.

[7]Hobson, G. V., and Lakshminarayana, B., "Prediction of Cascade Performance Using an Incompressible Navier-Stokes Technique," Gas Turbine and Aeroengine Congress and Exposition, American Society of Mechanical Engineers 90-GT-261, Brussels, Belgium, June 11–14, 1990.

[8]Ho, Y. K., Walker, G. J., and Stow, P., "Boundary Layer and Navier-Stokes Analysis of a NASA Controlled-Diffusion Compressor Blade," Gas Turbine and Aeroengine Congress and Exposition, American Society of Mechanical Engineers 90-GT-236, Brussels, Belgium, June 11–14, 1990.

[9]Sanger, N. L., and Shreeve, R. P., "Comparison of Calculated and Experimental Cascade Performance for Controlled Diffusion Compressor Stator Blading," *Journal of Turbomachinery*, Vol. 108,

1986, pp. 42–50.

[10]Murray, K. D., "Automation and Extension of LDV Measurements of Off-Design Flow in a Subsonic Cascade Wind Tunnel," A.E. Thesis, Naval Postgraduate School, Monterey, CA, 1989.

[11]Elazar, Y., "A Mapping of the Viscous Flow Behavior in a Controlled-Diffusion Compressor Cascade Using Laser Doppler Velocimetry and Preliminary Evaluation of Codes for the Prediction of Stall," Ph.D. Dissertation, Naval Postgraduate School, Monterey, CA, 1988.

[12]Tennekes, H., and Lumley, J. L., *A First Course in Turbulence*, MIT Press, Cambridge, MA, 1983.

[13]Hinze, J., *Turbulence*, McGraw-Hill, New York, 1975.

[14]Johnson, J. P., private communication, Nov. 30, 1990.

[15]Shreeve, R. P., Elazar, Y., Dreon, J. W., and Baydar, A., "Wake Measurements and Loss Evaluation in a Controlled Diffusion Compressor Cascade," Gas Turbine and Aeroengine Congress and Exposition, American Society of Mechanical Engineers 90-GT-129, Brussels, Belgium, June 1990.